2018 IEEE Intelligent Vehicles Symposium (IV)
Changshu, Suzhou, China, June 26-30, 2018

Emergency Autonomous Vehicle Guidance Under Steering Loss*

Mohamed Boudali, Rodolfo Orjuela, Michel Basset and Rachid Attia

***Abstract*— The autonomous vehicle guidance needs a steering system which is able to handle the lateral dynamics and a throttle/braking system to handle the longitudinal dynamics. However, a failure in the steering system leads the vehicle in dangerous situation. In order to manage this situation, an emergency guidance control architecture aims to guide and stop the vehicle in a safe area is proposed here. To that end, an emergency guidance controller (EGC) is developed to ensure the lateral guidance as well as the longitudinal guidance using braking torques. Since the same actuators (brakes) are employed for both control objectives a managing mechanism is proposed. Finally, simulation tests are carried out to show the effectiveness of the proposed approach.**

I. INTRODUCTION

Autonomous vehicles are considered as a promising way for intelligent transport systems as stated by members of the IEEE society[2]. In fact, the autonomous vehicle can help to improve the road safety, reduce the fuel consummation, optimize the infrastructure use and finally the mobility for all.

Generally, the control guidance is based on a control architecture comprising three main levels: perception, reference generation and control [1]. The perception level provides all informations related to the vehicle and its environment. The generation reference level uses the perception informations to provide two profiles: the geometric reference trajectory and the reference speed. Finally, the control level has to ensure the automated guidance along the generated references by providing appropriate control signals i.e. the steering angle δ for the lateral guidance and, the throttle and braking levels, $\%T$ and $\%B$ respectively, for the longitudinal guidance (see Figure 1). Due to the coupling of the vehicle dynamics, the automated guidance requires coupled longitudinal and lateral controllers as presented in [2]–[4]. However, the design of such controllers is more difficult due to the complexity of the vehicle dynamics. A way to cope with this problem is to consider a decoupled longitudinal and lateral controller designs. For example, a nested PID [5] and a state feedback [6], [7] are proposed for the lateral guidance. For the longitudinal guidance problem, a controller based on a sliding mode technique [8] and an active cruise control based on a gain-scheduling control technique [9] are developed. These works show interesting results for automated guidance in normal driving condition even at a high speed. Nevertheless, a failure of the steering system (e.g. steer-by-wire) leads the vehicle uncontrolled and the situation becomes dangerous.

To deal with this problem, an emergency control guidance architecture must be introduced in the global control guidance architecture as shown in Figure 1. To the best of authors' knowledge few works are related to the design of this emergency control guidance architecture. In this paper an emergency control guidance architecture is proposed which aims to guide and stop the vehicle in a safe area (hard shoulder) when a failure of the steering system is detected. This control architecture contains the same levels of the guidance control architecture described above (see Figure 1). In fact, it uses the perception level to provide emergency references which are used by the emergency guidance controller (EGC).

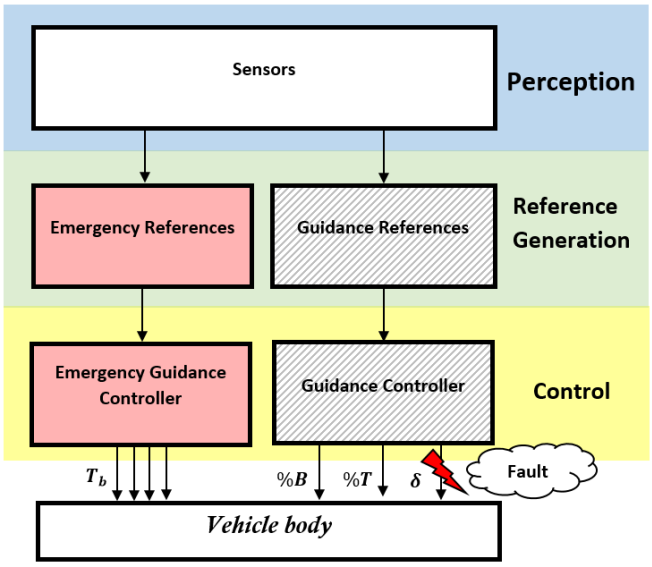

Fig. 1: Global control guidance architecture

The proposed EGC consists in a combined lateral and longitudinal controllers considering decoupled dynamics. In fact, the proposed EGC uses the braking torques T_b to simultaneously handle both lateral and longitudinal dynamics. Indeed, an appropriate braking torques are generated to stop the vehicle using a longitudinal controller. On the other hand, since the steering system is unavailable due to a failure, the lateral dynamics can be controlled

*This work was supported by Région d'Alsace and Mulhouse Alsace Agglomération (m2A).

Institut de Recherches en Informatique, Mathématiques, Automatique et Signal EA 7499, Université de Haute-Alsace, 12 rue des Frères Lumire F-68093 Mulhouse Cedex, France. firstname.lastname@uha.fr

[2]www.ieee.org/about/news/2012/5september_2_2012.html

using a differential braking. This differential braking generates a generalized guidance yaw moment M_z at the Center of Gravity (CoG) of the vehicle ensuring the lateral guidance. Let us remark that the generalized guidance yaw moment can be obtained using different combinations of the longitudinal tire forces and consequently an allocation control strategy becomes unavoidable [10], [11]. As both dynamics are handled using the same actuators i.e. brakes, a managing mechanism should be employed to avoid control conflicts between both objectives.

This paper is organized as follows. Vehicle dynamics modeled by nonlinear Two-Track model is presented in Section 2. Then the emergency guidance controller (EGC) development is detailed in Section 3. The performance and the feasibility of the proposed architecture are demonstrated through a simulation test in Section 4.

II. VEHICLE MODELING

This part is devoted to the vehicle dynamics modeling approximated by the nonlinear Two-Track model with coupled longitudinal and lateral forces. This model is described in the yaw plan by neglecting the roll dynamics and the load transfer.

The nonlinear Two-Track model is expressed by the following equations [12]:

$$\begin{aligned} m\dot{v}_x &= (F_{xfl} + F_{xfr})\, cos(\delta) + F_{xrl} + F_{xrr} \\ &- (F_{yfl} + F_{yfr})\, sin(\delta) + m\dot{\psi} v_y - F_{rr} \qquad (1) \\ m\dot{v}_y &= F_{yrl} + F_{yrr} + (F_{xfl} + F_{xfr})\, sin(\delta) \\ &+ (F_{yfl} + F_{yfr})\, cos(\delta) - m\dot{\psi} v_x \qquad (2) \\ I_z\ddot{\psi} &= L_f\,(F_{xfl} + F_{xfr})\, sin(\delta) + L_f\,(F_{yfl} \\ &+ F_{yfr})\, cos(\delta) - L_r\,(F_{yrl} + F_{yrr}) + \frac{L_w}{2}\,(F_{xfr} \\ &- F_{xfl})\, cos(\delta) + \frac{L_w}{2}\,(F_{xrr} - F_{xrl}) \\ &+ \frac{L_w}{2}\,(F_{yfl} - F_{yfr})\, sin(\delta) \qquad (3) \end{aligned}$$

where v_x and v_y are the longitudinal and the lateral velocities, the m and Iz denote the vehicle mass and the moment of inertia, L_f and L_r are the distances between the CoG and the front and the rear axles, L_w the track-width, δ is the steering wheel angle of the front wheels, F_x and F_y are the longitudinal and lateral forces and $i = \{fl, fr, rl, rr\}$ refer respectively to the $\{front, left\}$, $\{front, right\}$, $\{rear, left\}$ and $\{rear, right\}$ wheels.

The longitudinal and the lateral forces are function of the sideslip angle α_s and the longitudinal slip ratio λ as follows:

$$F_x = \mu_x\,(\lambda, \alpha_s, \mu)\, F_z \qquad (4)$$

$$F_y = \mu_y\,(\lambda, \alpha_s, \mu)\, F_z \qquad (5)$$

where F_z is the tire normal load, μ the road adhesion coefficient. The longitudinal and lateral forces are related through the friction circle relationship expressed by:

$$\sqrt{F_x^2 + F_y^2} \leq \mu F_z \qquad (6)$$

The rotational dynamics of each wheel are modeled by the same equation given by [13]:

$$J_w\dot{\omega}_i = T_{ti} - T_{bi} - RF_{xi} \qquad (7)$$

where ω_i the rotational velocity of the i wheel, J_w is the moment of inertia of the wheel, R the wheel radius, T_{ti} and T_{bi} denote the traction torque and the braking torque transmitted to the i wheel respectively. Here, each wheel is assumed can be individually braked.

All parameters used are summarized in Table I.

TABLE I: Vehicle model parameters

Symbol	Parameter	Value
m	Vehicle mass	$1700\,(kg)$
I_z	Vehicle inertia moment	$3048\,(kgm^2)$
I_w	Wheel inertia moment	$0.99\,(kgm^2)$
L_f	Front-CoG distance	$1.04\,(m)$
L_r	Rear-CoG distance	$1.65\,(m)$
L_w	Track width	$1.54\,(m)$
R	wheel radius	$0.31\,(m)$

III. EMERGENCY GUIDANCE CONTROLLER DESIGN

Once a total failure of the steering system is detected by the fault detection and isolation (FDI) supervisor, the EGC is enabled. Let us remark that FDI methods of the steering system based on sliding mode observer [14] and hybrid bond graph [15] are proposed. Their design is out of the scope of our contribution and here it is assumed that this supervisor is already designed. The task of the EGC is to guide the vehicle to a safe area (hard shoulder) and reduce the speed of the vehicle up to its stop. For this purpose, the proposed EGC consists in a combined lateral and longitudinal controllers considering decoupled dynamics as shown in Figure 2.

The lateral controller is based on a hierarchical control architecture comprising two levels: a high-level controller and a low-level controller. The high-level lateral controller (HLC) generates a generalized guidance yaw moment M_z at the CoG of the vehicle. An Optimal Control Allocation (OCA), particularly adapted to cope with over-actuated systems [10], [16], distributes this moment to obtain differential braking forces F_b. Finally, these forces are used by the low-level lateral controller (LLC) to provide appropriate braking torques $T_{b_i}^c$. On the other hand, the longitudinal controller based on a PID controller provides required braking torques $T_{b_i}^l$ to reduce the speed of the vehicle up to its stop. Since the same actuators (brakes) are used to ensure the lateral as well as the longitudinal guidances, the generated braking torques, $T_{b_i}^c$ and $T_{b_i}^l$, may be in competition and consequently control conflicts may

occur. To deal with this problem, a managing mechanism should be employed.

In this section, the design of both longitudinal and lateral controllers is detailed. The high level lateral controller, the optimal control allocation as well as the low level lateral controller are firstly presented. After then, the longitudinal controller based on a PID controller is investigated and finally the managing mechanism is discussed. The design of the FDI supervisor is outside of the focus of this paper and is assumed well available.

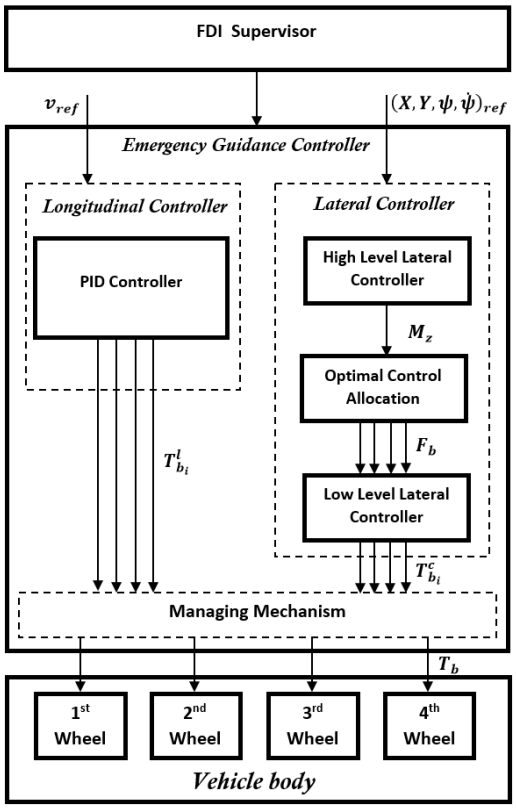

Fig. 2: Hierarchical control architecture of EGC

A. High-Level Lateral Controller

High-level lateral controller is designed using a 2DoF bicycle model with linear tire forces adding a direct yaw moment M_z as a control input [12]:

$$\begin{bmatrix} \dot{v}_y \\ \ddot{\psi} \end{bmatrix} = \begin{bmatrix} \frac{-a}{mv_x} & \frac{-b}{mv_x} - v_x \\ \frac{-b}{I_z v_x} & \frac{-c}{I_z v_x} \end{bmatrix} \begin{bmatrix} v_y \\ \dot{\psi} \end{bmatrix} + \begin{bmatrix} \frac{2C_f}{m} \\ \frac{2C_f L_f}{I_z} \end{bmatrix} \delta(t) + \begin{bmatrix} 0 \\ \\ \frac{1}{I_z} \end{bmatrix} M_z(t) \quad (8)$$

where

$$\begin{aligned} a &= 2\left(C_f + C_r\right) \\ b &= 2\left(C_f L_f - C_r L_r\right) \\ c &= 2\left(C_f L_f^2 + C_r L_r^2\right) \end{aligned}$$

C_f and C_r denote respectively the cornering stiffness of the front and the rear tires.

The lateral controller aims to minimize both the orientation error and the lateral error. The orientation error is defined between the longitudinal axis of the vehicle and the reference trajectory and is expressed as:

$$\dot{e}_\psi = \dot{\psi} - \dot{\psi}_{ref} \quad (9)$$

with $\dot{\psi}$ the yaw rate of the vehicle and $\dot{\psi}_{ref}$ the desired yaw rate. The lateral error dynamics defined between the CoG of the vehicle and the reference trajectory is given by [12]:

$$\dot{e}_y = v_y + v_x e_\psi \quad (10)$$

By using the equations (8), (10) and (9), the tracking error model can be written as:

$$\dot{\xi}(t) = A\xi(t) + BM_z(t) + D_1\dot{\psi}_{ref}(t) + D_2\delta(t) \quad (11)$$

with $\xi = [e_y, \dot{e}_y, e_\psi, \dot{e}_\psi]^T$ the state vector error and A, B, D_1 and D_2 the matrices such that:

$$\begin{aligned} A &= \begin{bmatrix} 0 & 1 & 0 & 0 \\ 0 & \frac{-a}{mv_x} & \frac{a}{m} & \frac{-b}{mv_x} \\ 0 & 0 & 0 & 1 \\ 0 & \frac{-b}{I_z v_x} & \frac{b}{I_z} & \frac{-c}{I_z v_x} \end{bmatrix}, B = \begin{bmatrix} 0 \\ 0 \\ 0 \\ \frac{1}{I_z} \end{bmatrix}, \\ D_1 &= \begin{bmatrix} 0 \\ \frac{-b}{mv_x} - v_x \\ 0 \\ \frac{-c}{Izv_x} \end{bmatrix} \text{ and } D_2 = \begin{bmatrix} 0 \\ \frac{2C_f}{m} \\ 0 \\ \frac{2C_f L_f}{I_z} \end{bmatrix} \end{aligned} \quad (12)$$

Notice that the high-level lateral controller calculates M_z to stabilize the tracking error model dynamics (11) by ensuring the convergence of the state vector error ξ towards zero. However, the model dynamics are disturbed by $\dot{\psi}_{ref}$ and δ, and therefore their impacts should be attenuated. To achieve these goals, a lateral controller consisting in a feedforward coupled to a robust state feedback is proposed:

$$M_z(t) = M_z^{FF}(t) + M_z^{FB}(t) \quad (13)$$

with M_z^{FF} and M_z^{FB} the feedforward and the robust state feedback actions respectively.

The feedforward action is obtained from (11) and (13) as follows:

$$M_z^{FF}(t) = -2C_f L_f \delta(t) + \frac{c}{v_x}\dot{\psi}_{ref}(t) \quad (14)$$

then the tracking error model (11) becomes:

$$\dot{\xi}(t) = A\xi(t) + BM_z^{FB}(t) + +D_1'\dot{\psi}_{ref}(t) + D_2'\delta(t) \quad (15)$$

with

$$D_1' = \begin{bmatrix} 0 \\ \frac{-b}{mv_x} - v_x \\ 0 \\ 0 \end{bmatrix} \text{ and } D_2' = \begin{bmatrix} 0 \\ \frac{2C_f}{m} \\ 0 \\ 0 \end{bmatrix} \quad (16)$$

It should be noted that due to the structure of the input matrix B of the model (11), the feedforward action

eliminates only the impact of $\dot{\psi}_{ref}$ and δ on the orientation error dynamics $\dot{e}_{\psi}$. However the lateral error dynamics $\dot{e}_y$ is still influenced and it is then necessary to reduce this influence using the robust state feedback.

The robust state feedback aims to guarantee the exponential convergence of the state vector ξ while ensuring an attenuation level of the influence of $\dot{\psi}_{ref}$ and δ. However, ensuring their simultaneously attenuation will be harder to reach with the only available input M_z. In our study only the influence of $\dot{\psi}_{ref}$ is attenuated. The considered robust state feedback is:

$$M_z^{FB}(t) = -K\xi(t) \tag{17}$$

with $K \in \mathbb{R}^{1\times 4}$ denoting the gain of the robust feedback to be calculated. By using the robust state feedback (17), the state space representation of the equation (15) becomes:

$$\dot{\xi}(t) = (A - BK)\,\xi(t) + D_1'\dot{\psi}_{ref}(t) + D_2'\delta(t) \tag{18}$$

The design of the robust feedback controller (17) is established using Lyapunov theory. For that purpose, the following condition must be held [17]:

$$\exists \alpha > 0 : \quad \dot{V}_{\xi}(t) + 2\alpha V_{\xi}(t) + z^T(t)z(t) - \gamma\dot{\psi}_{ref}^2(t) < 0 \tag{19}$$

with

$$V_{\xi}(t) = \xi^T(t)P\xi(t), \qquad P = P^T > 0 \tag{20}$$

$\alpha > 0$ the decay rate of the exponential convergence, $\gamma > 0$ the attenuation level and the vector z is the part of the state vector ξ influenced by $\dot{\psi}_{ref}$ such that:

$$z(t) = H\xi(t) \tag{21}$$

$||\beta||_2^2$ is the $\mathcal{L}_2$ norm of β and $H \in \mathbb{R}^{4\times 4}$ is a weighting matrix with an appropriate dimension.

Finally, the inequality (19) can be reformulated under the following linear matrix inequality (LMI) for a given α and γ:

$$\begin{bmatrix} C_{11}' & (HQ)^T \\ HQ & -\mathrm{I} \end{bmatrix} < 0 \tag{22}$$

with $C_{11}' = AQ + QA^T - BM - M^TB^T + 2\alpha Q + DD^T/\gamma$, $Q = P^{-1}$ and $M = KP^{-1}$. This LMI is obtained after some algebraic manipulation and applying the Schur complement [7]. The resolution of the LMI (22) consists then in finding the matrices Q and M for a given $\alpha > 0$ and $0 < \gamma < 1$. Finally, the gain of the robust state feedback is:

$$K = MQ^{-1} \tag{23}$$

Remark that a large decay rate α improve the convergence rate while $\gamma < 1$ reduces the impact of the disturbance on the target signal z. These two goals can not be satisfied simultaneously and consequently a trade-off between them is necessary. Note that the closed-loop performances (damping, etc.) can be improved by placing the poles of the error model in some specific regions, for example, a region defined by the intersection with a circle and a cone [18] and [19].

B. Optimal Control Allocation (OCA)

The optimal control allocation aims to distribute the generalized yaw moment M_z provided by the high-level lateral controller to the low-level controllers using an optimization algorithm. The optimizer calculates the braking forces by minimizing an objective function subject to constraints related to the physical limits of brakes. The OCA problem is formulated considering an individual wheel braking. The vector of braking forces F_b is calculated by solving the following optimization problem:

$$F_b^* = \arg\min_{F_b} || \; M_z - B_{ef}F_b \; || \tag{24}$$

where B_{ef} is the effectiveness matrix and F_b the vector of the braking forces. They are obtained from (3) and given by:

$$B_{ef} = \begin{bmatrix} b_1 & b_2 & L_w & -L_w \end{bmatrix} \in \mathbb{R}^{1\times 4} \tag{25}$$

with $b_1 = L_f \sin\delta + L_w \cos\delta$, $b_2 = L_f \sin\delta - L_w \cos\delta$ and the vector of braking forces:

$$F_b = \begin{bmatrix} F_{xfl} & F_{xfr} & F_{xrl} & F_{xrr} \end{bmatrix}^T \in \mathbb{R}^4 \tag{26}$$

subject to the physical constraints:

1) $F_b \leq 0$: the braking forces are negative.
2) $F_{b_{max}} \geq -F_b$ the maximum braking forces depends on the vertical load and satisfy the friction circle (6).

The constrained optimization problem can be solved using appropriate numerical algorithms. Among the available optimization algorithms, an interior point algorithm developed by [20] is used here.

C. Low-Level Lateral Controller

The low level lateral controller uses the longitudinal forces F_b provided by the OCA to calculate the physical control input. Here, the physical inputs are the braking torque for each wheel $T_{b_i}^c$. Our study is not focused on the low-level lateral controller design. However, a cotroller based on nonlinear output feedback control law for active braking control systems, such as proposed by [21], can employed.

D. Longitudinal Controller

The longitudinal controller aims to reduce the vehicle speed up to its stop. This controller tracks the speed reference $v_{x_{ref}}$ by providing appropriate braking torques. The generated braking torques must be limited to not exceed the physical limit of the actuators. To achieve this end, a saturated PID controller with anti-windup is used to obtain the following braking torque for each wheel:

$$T_{b_i}^l = \left(P + I\frac{1}{s} + D\frac{N}{1 + N\frac{1}{s}} \right) \left(v_x - v_{x_{ref}} \right) \tag{27}$$

the PID parameters are tuned to satisfy a damping less then 0.7 and a time response $112\,ms$. Notice that in the proposed

approach the same braking torque $T_{b_i}^l$ is applied on the four wheels in order to avoid creating an additional yaw moment that can impact the lateral dynamics. limit the impact of the longitudinal on the lateral guidance. For purposes of managing both the lateral braking torques $T_{b_i}^c$ and the longitudinal braking torques $T_{b_i}^l$, a managing mechanism is proposed.

E. Managing Mechanism

Both the lateral and longitudinal controllers provide braking torques, $T_{b_i}^c$ and $T_{b_i}^l$, to ensure a specific objective. As these braking torques should be applied to the same actuator, a combination of them should be done to generate a global braking torque as follows:

$$T_{b_i} = \alpha_b T_{b_i}^c + (1 - \alpha_b) T_{b_i}^l \tag{28}$$

where $\alpha_b \in [0, 1]$ is a weighting function. This weighting function help to manage both lateral and the longitudinal handling in order to avoid control conflicts between both objectives. According to its time-variation, more or less priority is given to the lateral or the longitudinal goals.

F. Emergency Reference Generation

The emergency reference generation provides a reference trajectory as well as a reference speed.

The *reference trajectory* is generated considering small curvatures and the path free of obstacles. These small curvatures are required to reduce the needed yaw moment M_z and consequently brake solicitations.

The *speed reference* is generated in order to be able to provide an enough yaw moment without saturating brakes. In fact, for the same yaw moment, the braking torques are less important at a high speed then that at a low speed. Generally speaking, the speed reference is constant at the beginning follows of progressive deceleration phases.

IV. SIMULATIONS

The EGC performance through a simulation test is carried out considering a total failure of the steering system at the time zero of the simulation. The failure is assumed well detected by the FDI supervisor and the emergency guidance control architecture is enabled. During the simulation test the brakes are supposed in good condition and no other sensors/actuators failures are considered. The initial speed is constant $v_{x_0} = 15\,m/s$ and the steering angle is assumed zero along all the trajectory.

The simulation results are shown on Figures 3 and 4. It can be noticed that the EGC offers good lateral guidance as well as longitudinal guidance performances. In fact, the tracking errors are admissible ($e_y \leq 10\,cm$ and $e_\psi = 1$ deg) and the vehicle is well stopped.

The longitudinal guidance is ensured by providing a braking torque $T_{b_i}^l$ for each wheel between $5\,s$ and $9\,s$ up to the vehicle stops. For the lateral guidance, an enough generalized yaw moment M_z between $1\,s$ and $6\,s$ is provided by the HLC. This M_z is distributed to differential braking

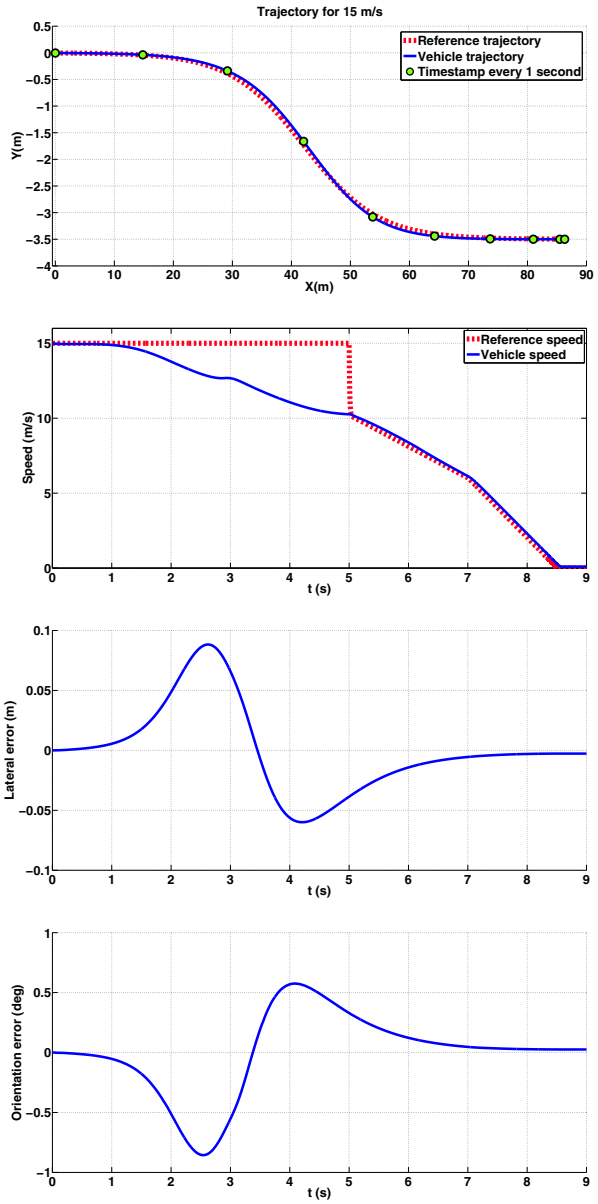

Fig. 3: Tracking results of the EGC

torques $T_{b_i}^c$ in such way that the right wheels are braked to turn left and then the left wheels are braked to turn right as shown in Figure 4. However, the differential braking torques influence the longitudinal dynamics and the vehicle speed is significantly reduced despite the reference speed is constant. It can be also seen that both braking torques for the lateral and the longitudinal guidance are well handled by the manging mechanism and particularly between $5\,s$ and $6\,s$.

In order to achieve the emergency guidance, a long distance ($d = 86\,m$) is needed for a lane change of $3.5\,m$. This distance can be reduced but at the expense of the differential braking torque $T_{b_i}^c$ needed for the lateral guidance. In fact, a short distance d involves a reference trajectory with large curvatures and consequently a large generalized yaw

moment.

V. CONCLUSIONS

In this paper, an emergency guidance control architecture is proposed. It aims to guide and stop the vehicle to a safe area when a total failure of the steering system is detected. The proposed architecture is based on a combined lateral and longitudinal controllers (EGC) using the same actuators (brakes). The longitudinal controller based on a PID controller provides braking torques for the longitudinal guidance, whereas the lateral controller, based on hierarchical control architecture, provides differential braking torques for the lateral guidance. The hierarchical control comprises two main levels: HLC and LLC. The HLC generates a generalized yaw moment which is distributed to the braking forces by the OCA. Afterwards, these forces are used by the LLC in order to provide differential braking torques. A managing mechanism to avoid conflict control between the longitudinal and the lateral guidance is proposed. The performance of the proposed EGC is shown through a simulation test.

In future works, a reconfiguration control of the EGC in the presence of the loss of the effectiveness of the brakes should be studied. Moreover, in order to ensure an optimal use of the brakes for the longitudinal guidance as well the lateral guidance, the managing mechanism should be optimized.

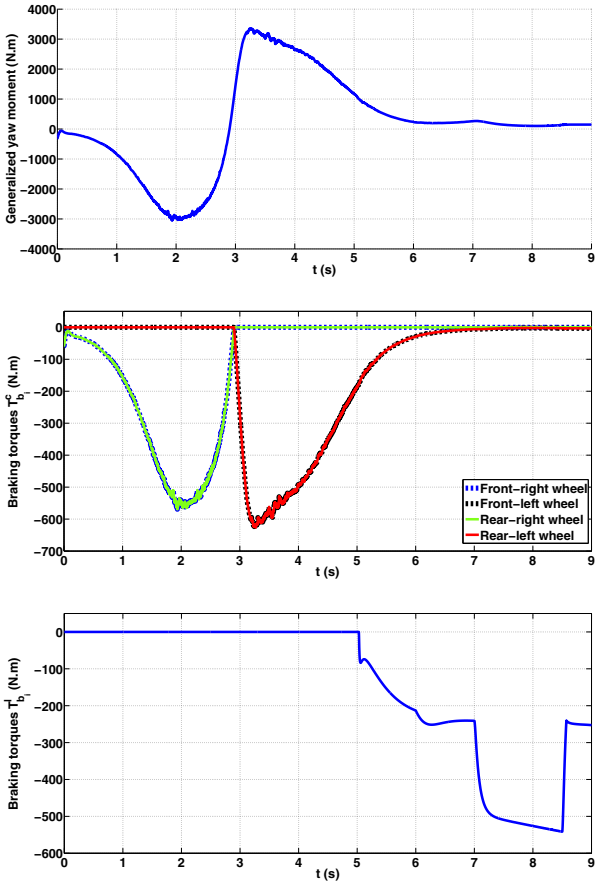

Fig. 4: Control actions results of the EGC

REFERENCES

[1] R. Attia, J. Daniel, J. P. Lauffenburger, R. Orjuela, and M. Basset, "Reference generation and control strategy for automated vehicle guidance," in *2012 IEEE Intelligent Vehicles Symposium*, (Spain), pp. 389–394, 2012.

[2] P. Falcone, F. Borrelli, J. Asgari, H. Tseng, and D. Hrovat, "Predictive Active Steering Control for Autonomous Vehicle Systems," *IEEE Transactions on Control Systems Technology*, vol. 15, no. 3, pp. 566–580, 2007.

[3] R. Attia, R. Orjuela, and M. Basset, "Combined longitudinal and lateral control for automated vehicle guidance," *Vehicle System Dynamics*, vol. 52, no. 2, pp. 261–279, 2014.

[4] P. Song, C. Zong, and M. Tomizuka, "Combined longitudinal and lateral control for automated lane guidance of full drive-by-wire vehicles," *SAE International Journal of Passenger Cars-Electronic and Electrical Systems*, vol. 8, no. 2, pp. 419–424, 2015.

[5] R. Marino, S. Scalzi, and M. Netto, "Nested PID steering control for lane keeping in autonomous vehicles," *Control Engineering Practice*, vol. 19, no. 12, pp. 1459–1467, 2011.

[6] N. Minoiu Enache, M. Netto, S. Mammar, and B. Lusetti, "Driver steering assistance for lane departure avoidance," *Control Engineering Practice*, vol. 17, no. 6, pp. 642–651, 2009.

[7] M. Boudali, R. Orjuela, and M. Basset, "A comparison of two guidance strategies for autonomous vehicles," in *20th IFAC World Congress*, (France), pp. 12539 – 12544, 2017.

[8] H. T. Luu, L. Nouvelire, and S. Mammar, "Dynamic programming for fuel consumption optimization on light vehicle," in *6th IFAC Symposium on Advances in Automotive Control*, (Germany), pp. 372 – 377, 2010.

[9] P. Shakouri, A. Ordys, D. Laila, and M. Askari, "Adaptive cruise control system: Comparing gain-scheduling PI and LQ controllers," in *18th IFAC World Congress*, (Italy), pp. 12964 – 12969, 2011.

[10] M. B. Alberding, J. Tjnns, and T. A. Johansen, "Nonlinear hierarchical control allocation for vehicle yaw stabilization and rollover prevention," in *2009 European Control Conference (ECC)*, (Hungary), pp. 4229–4234, 2009.

[11] R. Attia, R. Orjuela, and M. Basset, "Dual-mode control allocation for integrated chassis stabilization," in *19th IFAC World Congress*, (South Africa), pp. 11219 – 11224, 2014.

[12] R. Rajamani, *Vehicle Dynamics and Control*. Mechanical Engineering Series, Springer US, 2012.

[13] U. Kiencke and L. Nielsen, *Automotive Control Systems*. Springer, Berlin, Heidelberg, 2005.

[14] J. S. Im, F. Ozaki, T. K. Yeu, and S. Kawaji, "Model-based fault detection and isolation in steer-by-wire vehicle using sliding mode observer," *Mechanical Science and Technology*, vol. 23, no. 8, pp. 1991–1999, 2009.

[15] S. A. Arogeti, D. Wang, C. B. Low, and M. Yu, "Fault detection isolation and estimation in a vehicle steering system," *IEEE Transactions on Industrial Electronics*, vol. 59, no. 12, pp. 4810–4820, 2012.

[16] T. A. Johansen and T. I. Fossen, "Control allocation - A survey," *Automatica*, vol. 49, no. 5, pp. 1087 – 1103, 2013.

[17] S. P. Boyd, L. El Ghaoui, E. Feron, and V. Balakrishnan, *Linear matrix inequalities in system and control theory*. Society for Industrial and Applied Mathematics, 1994.

[18] M. Chilali, P. Gahinet, and P. Apkarian, "Robust pole placement in LMI regions," *IEEE Transactions on Automatic Control*, vol. 44, no. 12, pp. 2257–2270, 1999.

[19] S. Furuya and J. Irisawa, "LMI-based robust H2 control design with regional pole constraints for damping power system oscillations," *International Transactions on Electrical Energy Systems*, vol. 15, no. 1, pp. 13–29, 2005.

[20] O. Hrkegrd and S. T. Glad, "Resolving actuator redundancyoptimal control vs. control allocation," *Automatica*, vol. 41, no. 1, pp. 137 – 144, 2005.

[21] M. Tanelli, A. Astolfi, and S. M. Savaresi, "Robust nonlinear output feedback control for brake by wire control systems," *Automatica*, vol. 44, no. 4, pp. 1078 – 1087, 2008.